Malaya Journal of Matematik, Vol. 8, No. 2, 306-313, 2020

https://doi.org/10.26637/MJM0802/0002

Effect of constant heat source / sink on single component Marangoni convection in a composite layer bounded by adiabatic boundaries in presence of uniform & non uniform temperature gradients

R. Sumithra[1], R.K. Vanishree[2] and N. Manjunatha [3*]

Abstract

The Single component Marangoni convection is investigated in a composite layer, comprising of an incompressible single component fluid saturated porous layer over which lies a layer of same fluid with constant heat sources in both the layers. This composite layer is subjected to linear, parabolic and inverted parabolic temperature profiles. The upper boundary of the composite layer is free and the lower boundary is rigid and both the boundaries are adiabatic. A closed form solution is obtained for the thermal Marangoni numbers, which is an expression of various parameters. Effects of the physical parameters like porous parameter, Internal Rayleigh numbers in both the layers and thermal ratio on the thermal Marangoni Number investigated for all the three temperature profiles.

Keywords

Heat source, Marangoni convection, Temperature profiles and Marangoni number.

AMS Subject Classification: 76-XX,76Rxx,76Sxx.

[1] *Department of UG, PG Studies & Research in Mathematics, Government Science College Autonomous, Bengaluru,Karnataka, India;*
[2] *Department of Mathematics, Maharani's Science College for Women, Maharani Cluster University, Bengaluru, Karnataka, India;*
[3] *School of Applied Sciences, REVA University, Bengaluru, Karnataka, India.*
***Corresponding author**:[1]sumitra_diya@yahoo.com, [2]vanirkmscw@gmail.com, [3] manjunatha.n@reva.edu.in;
Article History: Received **10** December **2019**; Accepted **09** March **2020**

Contents

1 **Introduction** 306
2 **Formulation of the problem** 307
3 **Boundary Conditions** 308
4 **Method of Solution** 308
4.1 Linear temperature profile 308
4.2 Parabolic temperature profile 309
4.3 Inverted Parabolic temperature profile 309
5 **Results and Discussion** 310
6 **Conclusion** 312
References 312

1. Introduction

The Marangoni convection in a composite layer, subjected to additional effects has been given a lot of attention due to its applications in a variety of engineering and geophysical problems. The growth of crystals by various methods, oil recovery in petroleum industry and energy storage are some of other important application of the problem, where controlling convective instabilities is important, such instabilities can be controlled by maintaining a non uniform temperature gradients across the composite layer. These gradients are obtained by uniformly distributed internal heat sources or by injecting / removal of the fluid at one of the boundaries or by uniform heating and cooling at the boundaries.

Shivakumara *et al.* [8] has investigated the onset of surface-tension-driven space convection in a two layer system comprising an incompressible fluid-saturated porous layer over which lies a layer of same fluid by using regular perturbation technique. It was found that the depth ratio has a profound effect on the stability of the system. Liancum Zheng *et al.* [2] studied the Marangoni convection driven by a power law temperature gradient. They discussed the effects of various parameters on the velocity and temperature fields. Sumithra and Manjunatha [9] studied analytically the surface tension driven magneto convection in a composite layer bounded by

adiabatic boundaries. The different methods for modulation of Marangoni convection and Marangoni induced interface deformation in non-isotherm liquid films are studied by Tatiana [10]. Li and Yoda [11] have studied the Marangoni convection in a voltaic liquid film subjected to a horizontal temperature gradient confined in a rectangular cavity. Recently, Abdullah *et al.* [1] investigated the Marangoni convection in water-alumina nano fluid heated from below using a model which includes the effects of Brownian and thermopheric diffusions. They found that larger sized nano particles are unstable compared to nano particle of smaller average size. Giannetti *et al.* [4] investigated the numerical simulation of Marangoni convection within absorption aqueous Li-Br. They formulated a numerical model of the fundamental governing equations of vapour absorption in present of variable surface tension. Sankaran and Yarin [6] have studied the evaporation-driven thermocapillary Marangoni convection in liquid layers of different depths. They found that the velocity of thermocapillarity driven motion of tiny particles toward the cooler was predicted and found to be in reasonable agreement with the experimental result. Mahanthesh and Gireesha [3] studied the thermal Marangoni convection effects in Magneto-Cosson liquid flow through suspension of dust particles using Runge-Kutta-Fehlberg method. They found that the rate of heat transfer can be enhanced by suspending dust particles in a base liquid. Experimental and analytical tools have been used to study the effect of thermal Marangoni flux on the enhancement of oil recovery during immiscible injection in a matrix-fracture system by Abolhosseini *et al.* [5]. Siddheshwar and Vanishree [7] studied the Lorenz and Ginburg-Landau equations for thermal convection in a high-porosity medium with heat source. They showed that heat source has a significant influence on the heat transport.

In the present paper the composite layer is maintained by uniformly distributed internal heat source in both fluid and porous layers. Also, the composite layer is subjected to non uniform temperature gradients.

2. Formulation of the problem

Consider a horizontal single component, fluid saturated isotropic densely packed porous layer of thickness d_m underlying a single component fluid layer of thickness d with heat sources Q and Q_m respectively. The lower surface of the porous layer rigid and the upper surface of the fluid layer is free with surface tension effects depending on temperature. A Cartesian coordinate system is chosen with the origin at the interface between porous and fluid layers and the z-axis, vertically upwards. The basic equations governing such a system are,

$$\nabla.\overrightarrow{q} = 0 \tag{2.1}$$

$$\rho_0[\frac{\partial \overrightarrow{q}}{\partial t} + (\overrightarrow{q}.\nabla)\overrightarrow{q}] = -\nabla P + \mu\nabla^2\overrightarrow{q} \tag{2.2}$$

$$\frac{\partial T}{\partial t} + (\overrightarrow{q}.\nabla)T = \kappa\nabla^2 T + Q \tag{2.3}$$

$$\nabla_m.\overrightarrow{q_m} = 0 \tag{2.4}$$

$$\rho_0[\frac{1}{\varepsilon}\frac{\partial \overrightarrow{q_m}}{\partial t} + \frac{1}{\varepsilon^2}(\overrightarrow{q_m}.\nabla_m)\overrightarrow{q_m}] = -\nabla_m P_m - \frac{\mu}{K}\overrightarrow{q_m} \tag{2.5}$$

$$A\frac{\partial T_m}{\partial t} + (\overrightarrow{q_m}.\nabla_m)T_m = \kappa_m\nabla_m^2 T_m + Q_m \tag{2.6}$$

Where $\overrightarrow{q}$ velocity vector, ρ_0 fluid density, t time, μ fluid viscosity, P pressure, T temperature, constant heat source Q , κ thermal diffusivity of the fluid, ε is the porosity , K permeability of the porous medium, $A = \frac{(\rho_0 C_p)_m}{(\rho_0 C_p)_f}$ ratio of heat capacities, C_p specific heat, κ_m thermal diffusivity of the porous layer, Q_m is constant heat source for porous layer and the subscripts 'm' refer to the porous layer and 'f' refer to the fluid layer.

The basic state of fluid and porous layer is quiescent, have the following solutions

$$\overrightarrow{q} = \overrightarrow{q_b} = 0, P = P_b(z), T = T_b(z) \tag{2.7}$$

$$\overrightarrow{q_m} = \overrightarrow{q_{mb}}, P_m = P_{mb}(z_m), T_m = T_{mb}(z_m) \tag{2.8}$$

The temperature distributions $T_b(z)$ and $T_{mb}(z_m)$ are found to be

$$T_b(z) = \frac{-Qz(z-d)}{2\kappa} + \frac{(T_u - T_0)h(z)}{d} + T_0 \quad in \quad 0 \le z \le d \tag{2.9}$$

$$T_{mb}(z_m) = \frac{-Q_m z_m(z_m + d_m)}{2\kappa_m} + \frac{(T_0 - T_l)h_m(z_m)}{d_m} + T_0 \quad in \quad -d_m \le z_m \le 0 \tag{2.10}$$

where $T_0 = \frac{\kappa d_m T_u + \kappa_m d T_l}{\kappa d_m + \kappa_m d} + \frac{d d_m(Q_m d_m + Qd)}{2(\kappa d_m + \kappa_m d)}$ is the interface temperature and $h(z)$ and $h_m(z_m)$ are temperature gradients in fluid and porous layer respectively and subscript $'b'$ denote the basic state.

We superimpose infinitesimal disturbances on the basic state for fluid and porous layer respectively

$$\overrightarrow{q} = \overrightarrow{q_b} + \overrightarrow{q}', P = P_b + P', T = T_b(z) + \theta \tag{2.11}$$

$$\overrightarrow{q_m} = \overrightarrow{q_{mb}} + \overrightarrow{q_m}', P_m = P_{mb} + P_m', T_m = T_{mb}(z_m) + \theta_m \tag{2.12}$$

Where the prime indicates the perturbation. Introducing (2.11) and (2.12) in (2.1) - (2.6), operating curl twice and eliminate the pressure term from equations (2.2) and (2.5), the resulting equations then non dimensionalised.

The dimensionless equations are then subjected to normal mode analysis as follows

$$\begin{bmatrix} W \\ \theta \end{bmatrix} = \begin{bmatrix} W(z) \\ \theta(z) \end{bmatrix} f(x,y)e^{nt} \tag{2.13}$$

$$\begin{bmatrix} W_m \\ \theta_m \end{bmatrix} = \begin{bmatrix} W_m(z_m) \\ \theta_m(z_m) \end{bmatrix} f_m(x_m, y_m)e^{n_m t} \tag{2.14}$$

with $\nabla_2^2 f + a^2 f = 0$ and $\nabla_{2m}^2 f_m + a_m^2 f_m = 0$, where a and a_m are the wave numbers, n and n_m are the frequencies, W

and W_m are the dimensionless vertical velocities in fluid and porous layer respectively and obtain the following equations in $0 \le z \le 1$

$$(D^2 - a^2 + \frac{n}{Pr})(D^2 - a^2)W = 0 \quad (2.15)$$

$$(D^2 - a^2 + n)\theta + Wh(z) + R_I^*(2z-1)W = 0 \quad (2.16)$$

in $-1 \le z_m \le 0$

$$(D_m^2 - a_m^2)W_m = 0 \quad (2.17)$$

$$(D_m^2 - a_m^2 + An_m)\theta_m + W_m h_m(z_m) + R_{Im}^*(2z_m+1)W_m = 0 \quad (2.18)$$

where
Pr is the prandtl number, $R_I^* = \dfrac{R_I}{2(T_0 - T_u)}$, $R_{Im}^* = \dfrac{R_{Im}}{2(T_l - T_0)}$, R_I is the internal Rayleigh number for fluid layer and R_{Im} is the internal Rayleigh number for porous layer.
Assume that the present problem is satisfies the principle of exchange instability, so putting $n = n_m = 0$. We get in $0 \le z \le 1$ and $-1 \le z_m \le 0$ respectively

$$(D^2 - a^2)^2 W = 0 \quad (2.19)$$

$$(D^2 - a^2)\theta + Wh(z) + R_I^*(2z-1)W = 0 \quad (2.20)$$

$$(D_m^2 - a_m^2)W_m = 0 \quad (2.21)$$

$$(D_m^2 - a_m^2)\theta_m + W_m h_m(z_m) + R_{Im}^*(2z_m+1)W_m = 0 \quad (2.22)$$

3. Boundary Conditions

The boundary conditions are nondimensionalized and then subjected to normal mode expansion and are

$$\begin{aligned} D^2W(1) + Ma^2\theta(1) &= 0, \\ W(1) = 0, W_m(-1) = 0, \widehat{T}W(0) &= W_m(0), \\ \widehat{T}\widehat{d}^2(D^2 + a^2)W(0) &= (D_m^2 + a_m^2)W_m(0), \\ \widehat{T}\widehat{d}(D^3W(0) - 3a^2DW(0)) &= -\beta D_m W_m(0), \\ D\theta(1) = 0, \theta(0) &= \widehat{T}\theta_m(0), \\ D\theta(0) = D_m\theta_m(0), D_m\theta_m(-1) &= 0 \end{aligned} \quad (3.1)$$

where
$\widehat{T} = \dfrac{T_l - T_0}{T_0 - T_u}$ is the thermal ratio, $M = -\dfrac{\partial\sigma_t}{\partial T}\dfrac{(T_0 - T_u)d}{\mu\kappa}$ is the thermal Marangoni number, $\beta = \dfrac{d_m^2}{K}$ is the porous parameter and $\widehat{d} = \dfrac{d_m}{d}$ is the depth ratio.

4. Method of Solution

The solutions W and W_m are obtained by solving (2.19) and (2.21) using the boundary conditions (3.1)

$$W(z) = A_1[\cosh az + a_1 \sinh az + a_2 z\cosh az + a_3 z\sinh az] \quad (4.1)$$

$$W_m(z_m) = A_1[a_4\cosh a_m z_m + a_5 \sinh a_m z_m] \quad (4.2)$$

where
$a_1 = \dfrac{\beta a_m \coth a_m}{2a^3\widehat{d}}, a_2 = -1 - (a_1 + a_3)\tanh a,$
$a_3 = \dfrac{a_m^2 - a^2\widehat{d}^2}{a\widehat{d}^2}, a_4 = \widehat{T}, a_5 = \widehat{T}\coth a_m.$

4.1 Linear temperature profile

Here taking

$$h(z) = 1 \quad and \quad h_m(z_m) = 1 \quad (4.3)$$

Substituting equation (4.3) into (2.20) and (2.22), the temperature distributions θ and θ_m are obtained using the temperature boundary conditions, as follows

$$\theta(z) = A_1[c_1\cosh az + c_2\sinh az + g_1(z)] \quad (4.4)$$

$$\theta_m(z_m) = A_1[c_3\cosh a_m z_m + c_4\sinh a_m z_m + g_{1m}(z_m)] \quad (4.5)$$

where
$g_1(z) = A_1[\Delta_1 - \Delta_2 + \Delta_3 - \Delta_4], g_{1m}(z_m) = A_1[\Delta_5 - \Delta_6]$
$\Delta_1 = \dfrac{(2E_1 z + E_2 z^2)}{4a}(a_1\cosh az + \sinh az)$
$\Delta_2 = \dfrac{E_2 z}{4a^2}(\cosh az + a_1\sinh az)$
$\Delta_3 = \dfrac{(6a^2z^2E_1 + 4a^2z^3E_2 + 6E_2 z)}{24a^3}(a_3\cosh az + a_2\sinh az)$
$\Delta_4 = \dfrac{(E_1 z + E_2 z^2)}{4a^2}(a_2\cosh az + a_3\sinh az)$
$\Delta_5 = \dfrac{(2E_{1m}z_m + E_{2m}z_m^2)}{4a_m}(a_5\cosh a_m z_m + a_4\sinh a_m z_m)$
$\Delta_6 = \dfrac{E_{2m}z_m}{4a_m^2}(a_4\cosh a_m z_m + a_5\sinh a_m z_m)$
$E_1 = R_I^* - 1, E_2 = -2R_I^*, E_{1m} = -(R_{Im}^* + 1),$
$E_{2m} = -2R_{Im}^* c_1 = c_3\widehat{T}, c_2 = \frac{1}{a}(c_4 a_m + \delta_3 - \delta_2),$
$c_3 = \dfrac{\delta_8}{\delta_9}, c_4 = \dfrac{\delta_6}{\delta_7}, \delta_1 = -A_1[\Delta_7 + \Delta_8 + \Delta_9 + \Delta_{10}]$
$\Delta_7 = \dfrac{(2a^2E_1 + E_2(a^2-1))}{4a^2}(\cosh a + a_1\sinh a)$
$\Delta_8 = \dfrac{E_2 + 2E_1}{4a}(a_1\cosh a + \sinh a)$
$\Delta_9 = \dfrac{(3a^2-3)E_1 + (2a^2-3)E_2}{12a^2}(a_2\cosh a + a_3\sinh a)$
$\Delta_{10} = \dfrac{(a^2E_1 + E_2(a^2+1))}{4a^3}(a_3\cosh a + a_2\sinh a)$
$\delta_2 = A_1[\dfrac{(2a^2a_1 - aa_2)E_1 + (a_3 - a)E_2}{4a^3}]$
$\delta_3 = A_1[\dfrac{2E_{1m}a_5}{4a_m} - \dfrac{a_4E_{2m}}{4a_m^2}]$
$\delta_4 = -A_1[\Delta_{11} + \Delta_{12}]$
$\Delta_{11} = [\dfrac{E_{2m} - 2E_{1m}}{4} - \dfrac{E_{2m}}{4a_m^2}](a_4\cosh a_m - a_5\sinh a_m)$
$\Delta_{12} = [\dfrac{2E_{1m} - E_{2m}}{4a_m}](a_5\cosh a_m - a_4\sinh a_m)$
$\delta_5 = \delta_1 - (\delta_3 - \delta_2)\cosh a$
$\delta_6 = \delta_4 a\widehat{T}\sinh a + \delta_5 a_m\sinh a_m$
$\delta_7 = a_m\cosh a_m a\widehat{T}\sinh a + a_m^2\cosh a\sinh a_m$
$\delta_8 = \delta_4\cosh a - \delta_5\cosh a_m$

$\delta_9 = -a\cosh a_m \widehat{T}\sinh a - a_m \cosh a \sinh a_m$
From the boundary condition $(3.1)^1$, the thermal Marangoni number for the linear temperature profile is as follows

$$M_1 = \frac{-\Lambda_1}{a^2(c_1\cosh a + c_2\sinh a + \Lambda_2 + \Lambda_3)} \tag{4.6}$$

where
$\Lambda_1 = \Delta_{13} + \Delta_{14}$
$\Delta_{13} = a^2(\cosh a + a_1 \sinh a) + a_2(a^2\cosh a$
$\Delta_{14} = 2a\sinh a) + a_3(a^2\sinh a + 2a\cosh a)$
$\Lambda_2 = (\frac{E_2+2E_1}{4a})R_1 - \frac{E_2}{4a^2}R_2$
$R_1 = (a_1\cosh a + \sinh a)$
$R_2 = (\cosh a + a_1 \sinh a)$
$\Lambda_3 = \Delta_{15} - \Delta_{16}$
$\Delta_{15} = \frac{(4a^2E_2 + 6a^2E_1 + 6E_2)}{24a^3}(a_3\cosh a + a_2\sinh a)$
$\Delta_{16} = \frac{(E_2+E_1)}{4a^2}(a_3\sinh a + a_2\cosh a)$

4.2 Parabolic temperature profile

For the parabolic temperature profile

$$h(z) = 2z \quad and \quad h_m(z_m) = 2z_m \tag{4.7}$$

Substituting (4.7) into (2.20) and (2.22), The temperature distributions θ and θ_m are obtained using the temperature boundary conditions is as follows

$$\theta(z) = A_1[c_5\cosh az + c_6\sinh az + g_2(z)] \tag{4.8}$$
$$\theta_m(z_m) = A_1[c_7\cosh a_m z_m + c_8\sinh a_m z_m + g_{2m}(z_m)] \tag{4.9}$$

where
$g_2(z) = A_1[\Delta_{17} - \Delta_{18} + \Delta_{19} - \Delta_{20}]$
$g_{2m}(z_m) = A_1[\Delta_{21} - \Delta_{22}]$
$\Delta_{17} = \frac{(2E_3z + E_4z^2)}{4a}(a_1\cosh az + \sinh az)$
$\Delta_{18} = \frac{E_4 z}{4a^2}(\cosh az + a_1\sinh az)$
$\Delta_{19} = \frac{(6a^2z^2E_3 + 4a^2z^3E_4 + 6E_4z)}{24a^3}(a_3\cosh az + a_2\sinh az)$
$\Delta_{20} = \frac{(E_3z + E_4z^2)}{4a^2}(a_2\cosh az + a_3\sinh az)$
$\Delta_{21} = \frac{(2E_{3m}z_m + E_{4m}z_m^2)}{4a_m}(a_5\cosh a_m z_m + a_4\sinh a_m z_m)$
$\Delta_{22} = \frac{E_{4m}z_m}{4a_m^2}(a_4\cosh a_m z_m + a_5\sinh a_m z_m)$
$E_3 = R_I^*, E_4 = -2(R_I^*+1), E_{3m} = -R_{Im}^*,$
$E_{4m} = -2(R_{Im}^*+1) c_5 = c_7\widehat{T}, c_6 = \frac{1}{a}(c_8 a_m + \delta_{12} - \delta_{11}),$
$c_7 = \frac{\delta_{17}}{\delta_{18}}, c_8 = \frac{\delta_{15}}{\delta_{16}}$
$\delta_{10} = -A_1[\Delta_{23} + \Delta_{24} + \Delta_{25} + \Delta_{26}]$
$\Delta_{23} = \frac{(2a^2E_3 + E_4(a^2-1))}{4a^2}(\cosh a + a_1\sinh a)$
$\Delta_{24} = \frac{E_4 + 2E_3}{4a}(a_1\cosh a + \sinh a)$
$\Delta_{25} = \frac{(3a^2-3)E_3 + (2a^2-3)E_4}{12a^2}(a_2\cosh a + a_3\sinh a)$
$\Delta_{26} = \frac{(a^2E_3 + E_4(a^2+1))}{4a^3}(a_3\cosh a + a_2\sinh a)$
$\delta_{11} = A_1[\frac{(2a^2a_1 - aa_2)E_3 + (a_3 - a)E_4}{4a^3}]$
$\delta_{12} = A_1[\frac{2E_{3m}a_5}{4a_m} - \frac{a_4E_{4m}}{4a_m^2}]$
$\delta_{13} = -A_1[\Delta_{27} + \Delta_{28}]$
$\Delta_{27} = [\frac{E_{4m} - 2E_{3m}}{4} - \frac{E_{4m}}{4a_m^2}](a_4\cosh a_m - a_5\sinh a_m)$
$\Delta_{28} = [\frac{2E_{3m} - E_{4m}}{4a_m}](a_5\cosh a_m - a_4\sinh a_m)$
$\delta_{14} = \delta_{10} - (\delta_{12} - \delta_{11})\cosh a,$
$\delta_{15} = \delta_{13}a\widehat{T}\sinh a + \delta_{14}a_m\sinh a_m$
$\delta_{16} = a_m\cosh a_m a\widehat{T}\sinh a + a_m^2\cosh a\sinh a_m$
$\delta_{17} = \delta_{13}\cosh a - \delta_{14}\cosh a_m$
$\delta_{18} = -a\cosh a_m\widehat{T}\sinh a - a_m\cosh a\sinh a_m$
From the boundary condition $(3.1)^1$, the thermal Marangoni number for parabolic temperature profile is as follows

$$M_2 = \frac{-\Lambda_1}{a^2(c_5\cosh a + c_6\sinh a + \Lambda_4 + \Lambda_5)} \tag{4.10}$$

where
$\Lambda_4 = (\frac{(E_4+2E_3)}{4a})R_1 - \frac{E_4}{4a^2}R_2$
$\Lambda_5 = \Delta_{29} - \Delta_{30}$
$\Delta_{29} = \frac{(4a^2E_4 + 6a^2E_3 + 6E_4)}{24a^3}(a_3\cosh a + a_2\sinh a)$
$\Delta_{30} = \frac{(E_4+E_3)}{4a^2}(a_3\sinh a + a_2\cosh a)$

4.3 Inverted Parabolic temperature profile

Consider this profile

$$h(z) = 2(1-z) \quad and \quad h_m(z_m) = 2(1-z_m) \tag{4.11}$$

Substituting (4.11) into (2.20) and (2.22), The temperature distributions θ and θ_m are obtained using the temperature boundary conditions, as follows

$$\theta(z) = A_1[c_9\cosh az + c_{10}\sinh az + g_3(z)] \tag{4.12}$$
$$\theta_m(z_m) = A_1[c_{11}\cosh a_m z_m + c_{12}\sinh a_m z_m + g_{3m}(z_m)] \tag{4.13}$$

where
$g_3(z) = A_1[\Delta_{31} - \Delta_{32} + \Delta_{33} - \Delta_{34}]$
$g_{3m}(z_m) = A_1[\Delta_{35} - \Delta_{36}]$
$\Delta_{31} = \frac{(2E_5z + E_6z^2)}{4a}(a_1\cosh az + \sinh az)$
$\Delta_{32} = \frac{E_6 z}{4a^2}(\cosh az + a_1\sinh az)$
$\Delta_{33} = \frac{(6a^2z^2E_5 + 4a^2z^3E_6 + 6E_6z)}{24a^3}(a_3\cosh az + a_2\sinh az)$
$\Delta_{34} = \frac{(E_5z + E_6z^2)}{4a^2}(a_2\cosh az + a_3\sinh az)$
$\Delta_{35} = \frac{(2E_{5m}z_m + E_{6m}z_m^2)}{4a_m}(a_5\cosh a_m z_m + a_4\sinh a_m z_m)$
$\Delta_{36} = \frac{E_{6m}z_m}{4a_m^2}(a_4\cosh a_m z_m + a_5\sinh a_m z_m)$

$E_5 = R_I^* - 2, E_6 = 2(1-R_I^*), E_{5m} = -2 - R_{Im}^*$
$E_{6m} = 2(1-R_{Im}^*) c_9 = c_{11}\widehat{T}, c_{10} = \frac{1}{a}(c_{12}a_m + \delta_{22} - \delta_{21})$
$c_{11} = \dfrac{\delta_{26}}{\delta_{27}}, c_{12} = \dfrac{\delta_{24}}{\delta_{25}}$
$\delta_{19} = -A_1[\Delta_{37} + \Delta_{38} + \Delta_{39} + \Delta_{40}]$
$\Delta_{37} = \dfrac{(2a^2E_5 + E_6(a^2-1))}{4a^2}(\cosh a + a_1 \sinh a)$
$\Delta_{38} = \dfrac{E_6 + 2E_5}{4a}(a_1 \cosh a + \sinh a)$
$\Delta_{39} = \dfrac{(3a^2-3)E_5 + (2a^2-3)E_6}{12a^2}(a_2 \cosh a + a_3 \sinh a)$
$\Delta_{40} = \dfrac{(a^2E_5 + E_6(a^2+1))}{4a^3}(a_3 \cosh a + a_2 \sinh a)$
$\delta_{20} = -A_1[\Delta_{41} + \Delta_{42}]$
$\Delta_{41} = [\dfrac{E_{6m} - 2E_{5m}}{4} - \dfrac{E_{6m}}{4a_m^2}](a_4 \cosh a_m - a_5 \sinh a_m)$
$\Delta_{42} = [\dfrac{2E_{5m} - E_{6m}}{4a_m}](a_5 \cosh a_m - a_4 \sinh a_m)$
$\delta_{21} = A_1[\dfrac{(2a^2a_1 - aa_2)E_5 + (a_3 - a)E_6}{4a^3}]$
$\delta_{22} = A_1[\dfrac{2E_{5m}a_5}{4a_m} - \dfrac{a_4E_{6m}}{4a_m^2}]$
$\delta_{23} = \delta_{19} - (\delta_{22} - \delta_{21})\cosh a,$
$\delta_{24} = \delta_{20}a\widehat{T}\sinh a + \delta_{23}a_m \sinh a_m$
$\delta_{25} = a_m \cosh a_m a\widehat{T}\sinh a + a_m^2 \cosh a \sinh a_m$
$\delta_{26} = \delta_{20}\cosh a - \delta_{23}\cosh a_m$
$\delta_{27} = -a\cosh a_m \widehat{T}\sinh a - a_m \cosh a \sinh a_m$

From the boundary condition $(3.1)^1$, the thermal Marangoni number for inverted parabolic temperature profile is as follows

$$M_3 = -\frac{\Lambda_1}{a^2(c_9\cosh a + c_{10}\sinh a + \Lambda_6 + \Lambda_7)} \qquad (4.14)$$

where

$\Lambda_6 = (\dfrac{(E_6+2E_5)}{4a})R_1 - \dfrac{E_6}{4a^2}R_2$
$\Lambda_7 = \Delta_{43} - \Delta_{44}$
$\Delta_{43} = \dfrac{(4a^2E_6 + 6a^2E_5 + 6E_6)}{24a^3}(a_3\cosh a + a_2 \sinh a)$
$\Delta_{44} = \dfrac{(E_6+E_5)}{4a^2}(a_3 \sinh a + a_2 \cosh a)$

5. Results and Discussion

The thermal Marangoni numbers M_1, M_2 and M_3 for linear, parabolic and inverted parabolic temperature profiles respectively are obtained as an expression of the related parameters. The values of M_1, M_2 and M_3 are drawn against the values of depth ratio $\widehat{d} = \frac{d_m}{d}$. The larger values of $\widehat{d}$ mean, $\widehat{d} >> 1$ i.e., $d_m >> d$ i.e., porous layer dominant composite layers. While the smaller values of $\widehat{d}$ mean, $\widehat{d} << 1$ i.e., $d_m << d$ i.e., the fluid layer dominant composite layers. The thermal Marangoni numbers mainly depend on the horizontal wave number a, the porous parameter $\beta = \dfrac{d_m^2}{K}$, the internal Rayleigh numbers R_I for the fluid layer and R_{Im} for the porous layer which represent internal heat source (sink) and thermal ratio $\widehat{T}$. The variation of these on the thermal Marangoni number are represented graphically in the following figures for all the three temperature profiles for fixed values of $a = \beta = R_I = R_{Im} = \widehat{T} = 1$.

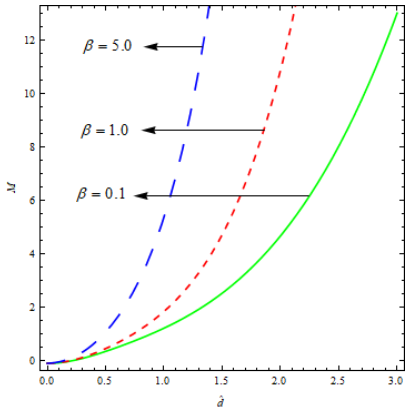

(a)

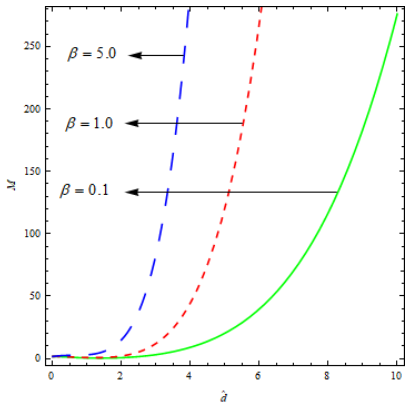

(b)

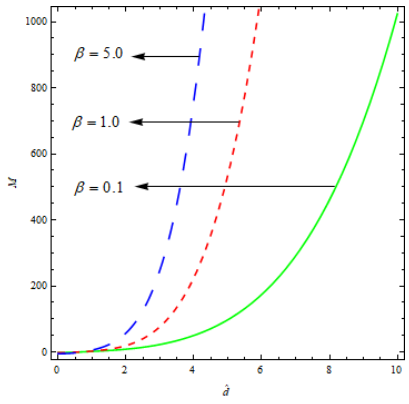

(c)

Figure 1. Effects of porous parameter β

The effects of the porous parameter β on the thermal Marangoni numbers M_1, M_2 and M_3 are depicted in figures 1a, 1b and 1c for the three temperature profiles namely, linear, parabolic and inverted parabolic temperature profiles respectively. It is evident from the figure that , the curves are diverging, indicating its effect is prominant for the porous layer dominant composite layer. Also, the values of $\beta = 0.1, 1.0, 5.0$, for a fixed value of depth ratio $\widehat{d}$, one can observe that

the increase in the value of β, raises the values of the thermal Marangoni numbers M_1, M_2, M_3 for all three profiles. i.e., the increase in the value of β stabilizes single component Maragoni number. From these figures we observe that $M_2(\beta) < M_1(\beta) < M_3(\beta)$ which clearly indicates that the heat transport is maximum for the inverted parabolic temperature profile.

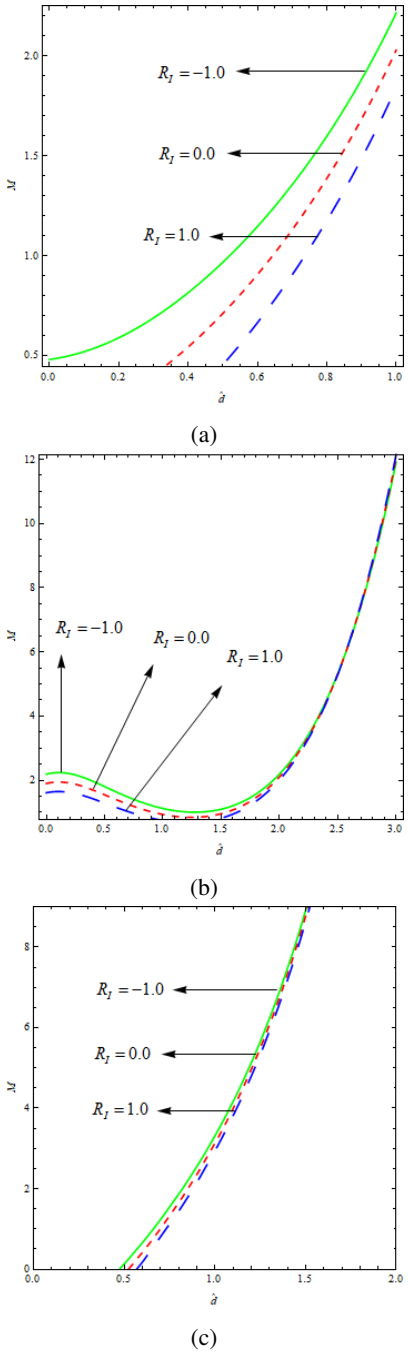

Figure 2. Effects of fluid internal Rayleigh number R_I

Figure 2a, b, c portray the effects of the internal Rayleigh number R_I, that is the effect of heat source / sink in the fluid layer, on the thermal Marangoni numbers, M_1, M_2 & M_3 for all three profiles. The curves are converging, which indicates its effect is drastic for smaller values of depth ratio, i.e., for fluid layer dominant composite layer. The values of R_I are $-1.0, 0.0$ &1.0 and for fixed value of depth ratio, the increase in the value of R_I, decreases the value of thermal Marangoni numbers for all the three profiles. This indicates that the decrease in the value of R_I stabilizes the single component Marangoni convection.

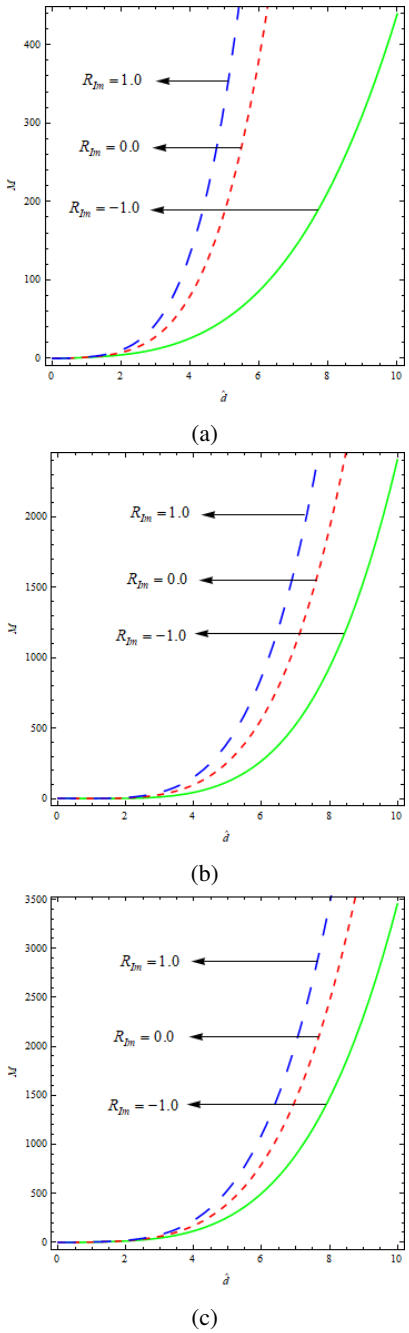

Figure 3. Effects of porous internal Rayleigh number R_{Im}

The effect of internal Rayleigh number R_{Im} that is the effect of heat source in the porous layer, on the thermal Marangoni

numbers M_1, M_2, M_3 is explained in the figure 3a, b, c, for all three temperature profiles linear, parabolic and inverted parabolic temperature profiles respectively. The values of R_{Im} taken are $-1.0, 0.0$ &1.0 and for a fixed depth ratio, the increase in the value of R_{Im} increases thermal Marangoni numbers. So, its effect is to stabilize the single component Marangoni convection. Also, the curves are diverging, depicting that the effect of R_{Im} is drastic for porous layer dominant composite layers as expected. From these figures we observe that the results with respect to R_{Im} are opposite to that of R_I. This is due to the fact that the increase in the depth ratio of porous layer stabilizes the system. The effect of thermal ratio $\widehat{T}$, which plays an important role in the convection problems, which takes into account of the boundary temperatures along with the interfacial temperature. Figure 4a, b, c show the effects of $\widehat{T}$ on the three thermal Marangoni numbers. The values of $\widehat{T}$ are $1.0, 1.5$ &2.0. For a fixed depth ratio, the increase in the value of $\widehat{T}$, is increasing the thermal Marangoni numbers for all the three profiles. The curves are diverging, which portrays that, the effect of $\widehat{T}$ is very important in the porous layer dominant composite layers. These results are qualitatively similar to that of R_{Im} and β.

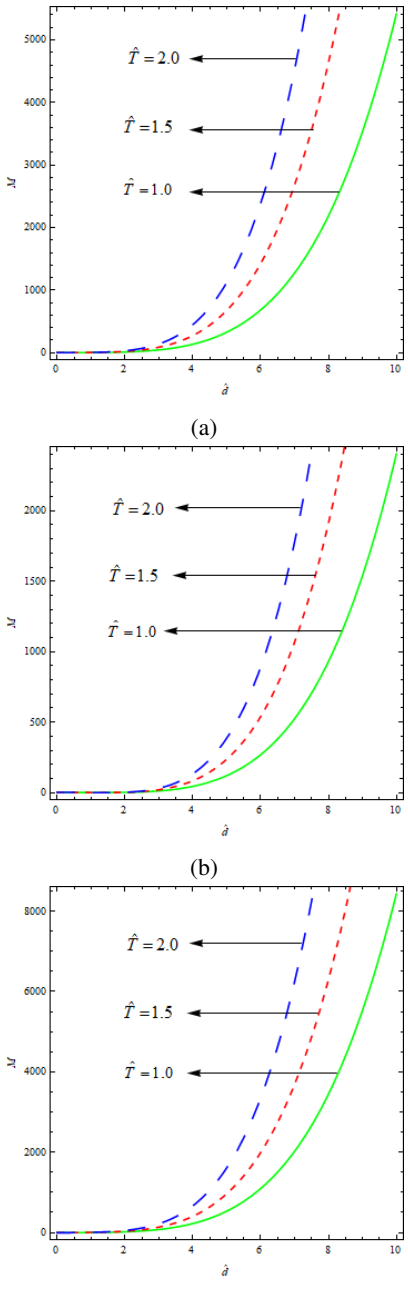

(a)

(b)

(c)

Figure 4. Effects of thermal ratio $\widehat{T}$

6. Conclusion

1. The inverted parabolic temperature profile is the most stabilising among the three temperature profile accomodated in this study. So, this profile is effective for the situations where convection has to be controlled, like crystal growths etc.
2. By increasing the values of β, R_{Im} & $\widehat{T}$ and decreasing the values of R_I, one can control Marangoni convection.
3. The effect of β, R_{Im} & $\widehat{T}$ are important for the porous layer dominant composite layers i.e., $d_m >> d$ and the effect of R_I is important for fluid layer dominant composite layer i.e., $d_m << d$. This is true for all the three temperature profiles.

Acknowledgment

The author Dr. N. Manjunatha, express his sincere thanks to the management of **REVA University**, Bengaluru, Karnataka, India for their encouragement and support.

References

[1] A.A. Abdullah, Marangoni convection in water-alumina nanofluids: Dependence on the nanoparticle size, *European journal of Mechanics-B/Fluids*, 67 (2018), 259–268.

[2] Liancun Zheng., Yanhai Lin and Xinxin Zhang, Marangoni convection of power law fluids driven by power-law temperature gradient, *Journal of the Franklin Institute*, 349(8)(2012), 2585–2597.

[3] B. Mahanthesha and B.J. Gireesha, Thermal Marangoni convection in two-phase flow of dusty Casson fluid, *Results in Physics*, 8(2018), 537–544.

[4] Niccolo Gianneti, Seiichi Yamaguchi and Kiyoshi Saito, Numerical simulation of Marangoni convection within absorptive aqueous Li-Br, *International Journal of Refrigeration*, 92(2018), 176–184.

[5] Pejman Abolhosseini, Maryam Khosravi, Behzad Rostami and Mohammad Masoudi, Influence of Thermal Marangoni convection on the recovery of by-passed oil during immiscible injection, *Journal of Petroleum Science and Engineering*, 164(2018), 196–205.

[6] A.Sankaran and A.L. Yarin, Evaporation-driven thermocapillary Marangoni convection in liquid layers of different depths, *International Journal of Heat and Mass Transfer*, 122(2018), 504–514.

[7] P.G. Siddheshwar and R.K.Vanishree, Lorenz and Ginzburg-Landau equations for thermal convection in a high-porosity medium with heat source, *Ain Shams J. Engg.*, 9(2018), 1547–1555.

[8] I.S. Shivakumara, JinhoLee and Krishna B. Chavaraddi, Onset of surface tension driven convection in a fluid layer overlying a layer of an anisotropic porous medium, *International Journal of Heat and Mass Transfer*, 54(4) (2011), 994–1001.

[9] R. Sumithra R and N. Manjunatha, Analytical study of surface tension driven magneto convection in a composite layer bounded by adiabatic boundaries, *International Journal of Engineering and Innovative Technology*, 1(6)(2012), 249–257.

[10] Tatiana Gambaryam-Roisman, historical prespective Modulation of Marangoni convection in liquid films, *Advances in Colloid and Interface Science*, 222(2015), 319–331.

[11] Yaofa Li and Minami Yoda, An experimental study of buoyancy-Marangoni convection in confined and volatile binary fluids, *International Journal of Heat and Mass Transfer*, 102(2016), 369–380.

★★★★★★★★★
ISSN(P):2319 – 3786
Malaya Journal of Matematik
ISSN(O):2321 – 5666
★★★★★★★★★